Desalination and Water Treatment
www.deswater.com

doi: 10.5004/dwt.2021.26898

217 (2021) 232–242
March

Optimization studies on culture conditions of the functional microbes to improve Cr(VI) removal efficiency using the response surface methodology

Xiao Yan[a,b,c], Jianlei Wang[a,b], Mingjiang Zhang[a,b], Juan Zhong[a,b], Daozhi Ma[a,b,c], Chuiyun Tang[a,b,c], Xuewu Hu[a,b,c,d], Xingyu Liu[a,b,*]

[a]*National Engineering Laboratory of Biohydrometallurgy, GRINM Group Corporation Limited, No. 11 XingKeDongda Str., Huairou District, Beijing 101407, China, Tel. +86 10 60662785; Fax: +86 10 60662789; emails: wellwoodliu@163.com (X. Liu), yx1443349211@163.com (X. Yan), wangjl201314@163.com (J. Wang), zmj0630@163.com (M. Zhang), 15707332838@163.com (J. Zhong), 1046433955@qq.com (D. Ma), 799910541@qq.com (C. Tang), huxuewu9@163.com (X. Hu)*
[b]*GRINM Resources and Environment Tech. Co., Ltd., Beijing 100088, China*
[c]*General Research Institute for Nonferrous Metals, Beijing 100088, China*
[d]*School of Metallurgical and Ecological Engineering, University of Science and Technology Beijing, Beijing 100083, China*

Received 30 June 2020; Accepted 1 December 2020

ABSTRACT

In this study, the contribution of impact factors of functional microbes on Cr(VI) removal was ranked by Plackett–Burman experiments. The optimization of the more sensitive factors, such as carbon source, inoculation percent, temperature, and pH, was conducted to improve removal rate of Cr(VI) through Box–Behnken design of response surface methodology. The maximum removal rate over 90.84% and microbial optical density (OD_{600}) over 1.36 were obtained under the optimal culture conditions of carbon source of 1.8 $g.L^{-1}$, and inoculation percent (v/v) of 10% when pH at 8.0 and temperature at 30°C. Microscopic characterization and energy spectrum analysis of products by scanning electron microscopy-energy dispersive spectrometer and X-ray photoelectron spectroscopy confirmed that Cr(VI) in water-solution was effective stabilized and reduced to Cr(III)-precipitation by bioremediation. In addition, the variation of microbial community structure revealed that removal rate of Cr(VI) varied greatly in conjunction with different microbial species. Our findings showed that the most predominant species was *Bacillus megaterium* increasing to 84.96%, followed by *Pseudomonas putida*, *Stenotrophomonas maltophilia*, and *Ochrobactrum* sp. Optimization research opens a major potential avenue for Cr(VI) removal, which could quickly reduce environmental and economic concerns.

Keywords: Chromium pollution; Toxicity; Optimization; Bioremediation; Precipitated products

1. Introduction

Chromium(Cr) pollution and its negative impact on ecology system have gained substantial concerns around the world. Therefore, researchers are trying to develop an efficient technology for removal Cr pollution [1]. As the common states in the natural environment, Cr(III) and Cr(VI) have a great difference in mobility, bioavailability, and toxicological properties [2]. Cr(III) is considered to be stable and non-toxic in nature environment. Also, Cr(III) plays a positive role in maintaining the blood glucose level, and decreasing body fat, cholesterol, and triglyceride

* Corresponding author.

levels [1,3]. However, Cr(VI) is considered highly toxic, solubility, and bioavailability as it causes severe ill effects on human and animal health [4]. Therefore, it is urgent to screen a cost-efficiency and eco-friendly method for conversion Cr(VI) to Cr(III) [1,5]. In recent years, removal of Cr(VI) is through various physical, chemical, and biological method [3]. Of these, bioremediation by microorganisms is widely concerned for removal Cr(VI) [1,2]. Xu et al. [6] concluded *Deinococcus radiodurans* R1 showed around 25.1% Cr(VI) reduction under *in-vitro* conditions in the initial 500 μm Cr(VI). In addition, González et al. [5] isolated a native bacteria (*Serratia* sp. C8.) from tannery sediments located in Elena, and this strain could reduce 80% of 20 mg L^{-1} Cr(VI) [5]. However, a harsh environment and poor nutrition might lead to the lower activity and population of the functional microorganisms, and cause a negative impact on Cr(VI) removal in bioremediation [7].

In order to enhance Cr(VI) removal efficiency and achieve long-term bioremediation, it is necessary to optimize the nutrients and culture conditions of functional microorganisms [8]. Previous studies have summarized the influence factors including carbon source, nitrogen source, pH, temperature, etc. [9,10]. It may cause negative effect such as low biological activity, rare microbial species, and long remediation cycle due to the lack of optimization process for variables [11,12]. Based on the above problems, more attentions are given to optimize sensitive factors to improve Cr(VI) removal efficiency [1,8]. Sathishkumar et al. [13] investigated the reduction rate by *Pseudomonas stutzeri* L1 and *Acinetobacter baumannii* L2 was up 97% and 99% under the optimal conditions for 24 d [13]. Therefore, it is necessary to optimize the more sensitive factors for improving Cr(VI) removal by microorganisms.

Various methods such as response surface methodology (RSM) can be used as a very significant statistical tool that can be efficiently used for optimization of bioremediation process [14]. It not only avoid "change-one-factor-at-a-time" in the traditional method, but also increase mathematical and statistical techniques [15,16]. The aim of RSM is to find out optimum response which is influenced by several independent variables [17]. Box–Behnken design (BBD), as the type model of RSM, has been used to design and evaluate the interactive effects of experimental variables [18,19]. Previous studies have been reported RSM-BBD to optimize for degradation of organic pollutants [20]. However, RSM-BBD for improving Cr(VI) removal by optimizing sensitive factors of functional microorganisms, is rarely studied. This is one explain that lower activity, less population, and slower metabolism of microorganisms in the natural environment lead to poor Cr(VI) removal during bioremediation before optimization experiments [21,22]. Moreover, few have focused on the relationship between Cr(VI) removal and microbial community succession, and which microbial species was the most contributor during bioremediation.

Therefore, the objective of this study to improve Cr(VI) removal efficiency by optimization experiment of RSM-BBD, explore the bioremediation mechanisms of Cr(VI), and reveal microbial community succession during bioremediation. The paper also highlights potential use of functional microorganisms for bioremediation of Cr(VI) under *in-situ* condition.

2. Materials and methods

2.1. Microorganism and media

The functional microbes (YX-CM) using this study, *S. maltophilia*, *Ochrobactrum* sp., *Bacillus megaterium* strain, and *Pseudomonas putida*, were isolated from a chromite factory (36°30′N, 101°51′E) in Qinghai province, China.

The YX-CM was cultured in Erlenmeyer conical flasks (300 mL), each holding 100 mL of Nutrient Broth (NB) for enrichment having the medium composition as (g L^{-1}): 6 tryptone, 3 yeast extract, 6 NaCl, 0.5$MgSO_4 \cdot H_2O$, 0.5K_2HPO_4, pH 8.0, and was sterilized at 121°C for 30 min. 0.1415 g of $K_2Cr_2O_7$, as the source of Cr(VI), was added into 1 L of medium, and its initial concentration is 50 mg.L^{-1}. All experimental groups were maintained at 25°C ± 2°C in a rotary shaker at 120 rpm for rejuvenation of microbes. Then, the microbial optical density (OD_{600}) was up to 0.4 for further investigation.

2.2. Cr(VI) removal experiments

A set of experiments were performed to assess the contribution of various factors to remove Cr(VI). After enrichment culture, the YX-CM was inoculated into the fresh medium with independent variation factors in Erlenmeyer conical flasks (250 mL). All experimental groups were cultivated into a rotary shaker with 120 rpm at 25°C for 15 d. 5 mL of samples in different experimental groups were taken to analyze the residual Cr(VI) by the 1.5 diphenylcarbazide method using a UV/vis spectrophotometer (TU-1810, and Puxitech, China) at the wavelength γ = 540 nm, and the microbial optical density was detected at the wavelength 600 nm. The removal rate of Cr(VI) was calculated according to the following formula:

$$\eta = \frac{C_0 - C_i}{C_0} \times 100\% \quad (1)$$

where η is the removal rate of Cr(VI), C_0 is the initial concentration, C_i is the concentration after 15 d.

2.3. Plackett–Burman design

According to microbial self-nutrition types and culture conditions, the carbon source, nitrogen source, pH, temperature, inoculation size, rotational speed, and salinity percent were selected. The relative importance of factors on Cr(VI) removal were screen out and evaluated vis the Plackett–Burman design. The details information of parameters is listed in Table 1.

2.4. BBD-RSM experiments

Based on the results of Plackett–Burman design, and the path of steepest ascent experiment, Design Expert software 8 (Stat-Ease, Int. Co., Minneapolis, MN, USA) was applied for optimization experiments of sensitive factors by response surface method (RSM). The levels of different process variables of all the experimental were shown in Table 2. A 29-run BBD in RSM with four factors and three

Table 1
Experimental parameters in two levels used for Cr(VI) removal by YX-CM using Placket–Burman design

Parameter	Symbol	Experimental value	
	Code	Lower	Higher
Carbon source (g L^{-1})	X_1	0.6	3.0
Nitrogen source (g L^{-1})	X_2	0.4	1.2
pH	X_3	7	11
Temperature (°C)	X_4	20	40
Rotational speed (rpm)	X_5	80	160
Inoculation size (v/v) (%)	X_6	5	15
Salinity percent (%)	X_7	2	6

Table 2
Selected parameters at different levels used for Cr(VI) removal in experimental groups

Factor	Parameter	Level		
		Low	Center	High
A	Carbon source (g L^{-1})	0.6	1.8	3.0
B	pH	6	8	10
C	Temperature (°C)	20	30	40
D	Inoculation percent (v/v, %)	5	10	15

levels, was conducted to analyze and optimize the levels of sensitive factors and interaction effects between various culture conditions which could influence the removal rate of Cr(IV) (Table 3). For statistical estimation, the various variables were determined according to the following equation:

$$x_i = \frac{\left(X_i - X_0\right)}{\Delta X_i} \tag{2}$$

where x_i was value of the independent variable, X_i was the actual value of the independent variable, X_0 was the actual value of X_i at the center-point, and ΔX_i was the value of the step change.

The response Y obtained was analyzed by multiple regression to fit the following second-order polynomial model:

$$Y = \beta_0 + \sum \beta_i x_i + \sum \beta_{ii} x_i^2 + \sum \beta_{ij} x_i x_j \tag{3}$$

where Y was the predicted response (the removal rate of Cr(IV)), x_i and x_j were the coded independent variables affecting the Y, β_0 was an intercept, and β_i, β_{ii}, and β_{ij} were the coefficients of the *i*th linear, quadratic, and interactive terms, respectively.

The significance of factors and their interactions in the model were evaluated by ANOVA analysis, and the significance level was identified 0.05. Then, the optimization of different factors was served to enhance the removal rate of Cr(VI) by desirability function.

2.5. Model validation

Two independent bioremediation of Cr(VI) experiments were carried out under the optimal conditions obtained from RSM-BBD to verify the consistency between the model prediction and the actual experiments.

2.6. Microbial community structures analysis

The DNA of experimental groups were extracted at regular time interval of 5 d using the E.Z.N.ATM Mag-Bind bacterial DNA kit (OMEGA, D5625-01) according to the manufacturer's instruction. The amplification and library preparation of the V3–V4 region of the 16S rRNA gene was performed. In the design, the 27F/1492R primers complementary to the up and down stream of V3–V4 was considered as the templates. To ensure the quality of the sequence, the sequence length, and nucleotide ambiguity were screened. Simultaneously, the reads of sequencing (forward, reverse) were combined by FLASH 2. A range of reads from 150 to 600 bp were reserved in the sequencing process. After all steps, the sequencing data were analyzed to detect microbial community structure [23].

2.7. Characterization of products

To explore the further mechanisms of Cr(VI) removal, the precipitated products after bioremediation were characterized by scanning electron microscopy-energy dispersive X-ray spectroscopy (SEM-EDS) and X-ray photoelectron spectroscopy (XPS) analysis. For SEM, the detailed steps were listed as following: the precipitated products were centrifuged at 6,600 rpm for 16 min and fixed using 2.5% (v/v) glutaraldehyde in phosphate buffer solution (PBS 0.1 M 8.0) for 12 h, then, after washing repeatedly by PBS, the samples were carried out dehydration experiment by ethanol solution with gradient concentration (30%, 50%, 70%, 90%, 95%, and 100%) for 14 min at each stage. Thereafter, samples were dried with dry ice, fixed on an aluminum stub, and coated with gold before observation by SEM at 200 kV (Jeol-840A, Japan). The main elements of precipitated products were analyzed by EDS. The variation in the chemical valence of the precipitated products was identified by XPS analysis. After being dried and ground, samples were fully laid on a 0.5 cm × 0.5 cm double-sided tape, attached to aluminum foil, and fixed between two flat stainless steel modules. Then, the samples were placed in a instrument for testing. XPS analysis was carried out using an Escalab 250Xi X-ray photoelectron spectrometer with monochromatic Al Kα (h_t = 1,486.6 eV) X-ray radiation [24].

3. Results and discussion

3.1. Contribution of the main factors of YX-CM for removal Cr(VI)

The contribution of different variation factors for Cr(VI) removal were screened and shown in Table 4. A larger gaps ranging from (18.20 ± 0.89)% to (79.09 ± 2.07)% suggested that various factors with different levels had an significant influence on Cr(VI) removal. The result is

Table 3
Experimental plan based on BBD and results of Cr(VI) removal rate

Run	Experimental value				Cr(VI) removal (%)	
	Carbon source ($g.L^{-1}$)	pH	Temperature (°C)	Inoculation percent (v/v) (%)	Experimental	Predicted
1	0.60	6.00	30	10.00	63.96	62.47
2	3.00	6.00	30	10.00	73.84	73.45
3	0.60	10.00	30	10.00	70.36	69.07
4	3.00	10.00	30	10.00	76.28	76.09
5	1.80	8.00	20	5.00	71.88	65.84
6	1.80	8.00	40	5.00	66.52	59.59
7	1.80	8.00	20	15.00	73.28	79.19
8	1.80	8.00	40	15.00	69.24	72.94
9	0.60	8.00	30	5.00	49.72	56.44
10	3.00	8.00	30	5.00	62.68	65.44
11	0.60	8.00	30	15.00	75.2	69.78
12	3.00	8.00	30	15.00	86.52	78.78
13	1.80	6.00	20	10.00	78.16	79.30
14	1.80	10.00	20	10.00	73.6	71.05
15	1.80	6.00	40	10.00	59.48	60.19
16	1.80	10.00	40	10.00	80.64	77.66
17	0.60	8.00	20	10.00	71.6	70.29
18	3.00	8.00	20	10.00	76.44	79.29
19	0.60	8.00	40	10.00	61.24	64.03
20	3.00	8.00	40	10.00	70.32	73.03
21	1.80	6.00	30	5.00	58.44	59.02
22	1.80	10.00	30	5.00	60.72	63.63
23	1.80	6.00	30	15.00	72.92	72.37
24	1.80	10.00	30	15.00	72.88	76.98
25	1.80	8.00	30	10.00	90.84	88.59
26	1.80	8.00	30	10.00	85.6	86.56
27	1.80	8.00	30	10.00	83.2	84.56
28	1.80	8.00	30	10.00	89.52	87.96
29	1.80	8.00	30	10.00	88.64	87.56

Table 4
Twelve-trial Placket–Burman design matrix for seven variables with coded values along with observed removal rate of Cr(VI)

Run	Carbon source ($g.L^{-1}$)	Nitrogen source ($g.L^{-1}$)	pH	Temperature (°C)	Rotation rate (rpm)	Inoculation size (%)	Salinity ($g\ L^{-1}$)	Removal rate of Cr(VI) (%)
1	0.6	1.2	11	20	80	5	6	52.19 ± 1.32
2	0.6	1.2	11	20	160	15	6	79.09 ± 2.07
3	0.6	0.4	7	40	160	15	6	73.50 ± 1.99
4	3.0	1.2	7	20	160	15	2	74.81 ± 1.76
5	0.6	0.4	11	40	80	15	2	61.20 ± 1.23
6	3.0	1.2	11	40	80	15	2	66.09 ± 1.90
7	0.6	1.2	7	40	160	5	2	69.35 ± 2.08
8	0.6	0.4	7	20	80	5	2	60.40 ± 2.11
9	3.0	0.4	7	20	80	15	6	55.88 ± 1.51
10	0.6	1.2	7	40	80	5	6	27.36 ± 1.09
11	3.0	0.4	11	20	160	5	2	18.20 ± 0.89
12	3.0	0.4	11	40	160	5	6	32.45 ± 0.27

summarized in Fig. 1, the carbon source, pH, temperature, and inoculation size were found the relative significant for Cr(VI) removal rate.

As the necessary nutrients, carbon source had a positive effect on population and activity of the functional microorganisms. Chen et al. [25] confirmed that adequate nutrients contributed to increasing Cr(VI) removal efficiency by improving population and activity of functional microorganisms during bioremediation. Moreover, previous studies have believed carbon source by supplying electrons can aid to reduce Cr(VI) to Cr(III) [26,27]. Therefore, it was relative reasonable that carbon source was the most sensitive factor affecting Cr(VI) removal of bioremediation.

It was important to detect inoculation percent had an significant effect on Cr(VI) removal. The removal rate varied significantly in conjunction with inoculation percent increased greatly from 5% to 15% (v/v). In fact, the higher inoculation size can effectively improve microbial reproduction and metabolism in the bioremediation systems. Therefore, compelling microorganisms to resist harsh environment rapidly by bioremediation Cr(VI) rather than continuing to maintain adaptation period [28].

The temperature was controlling the growth of microorganisms and Cr(VI) reductase activity. Too lower or higher temperature had an adverse influence on the Cr(VI) removal. Previous studies reductase inactivation of bioremediation systems can be attributed to the unsuitable temperature [5]. In addition, with the increasing of temperature from 40°C to 50°C, the poor microbial population and activity led to the low removal rate [29].

The pH was also a sensitive factor in the bioremediation process of Cr(VI). First, a negative correlation between extreme pH and Cr(VI) bioremediation has been well proved in the previous studies [8]. The lower pH (<4) caused the desorption and oxidization of chromium after biosorption, whereas at higher pH (>10) affected microbial activity and population [16]. Therefore, it was necessary to optimize the pH of functional microorganisms during bioremediation. Shahid et al. [1] observed the important relationship between pH and the population and activity of microorganisms on Cr(VI) removal.

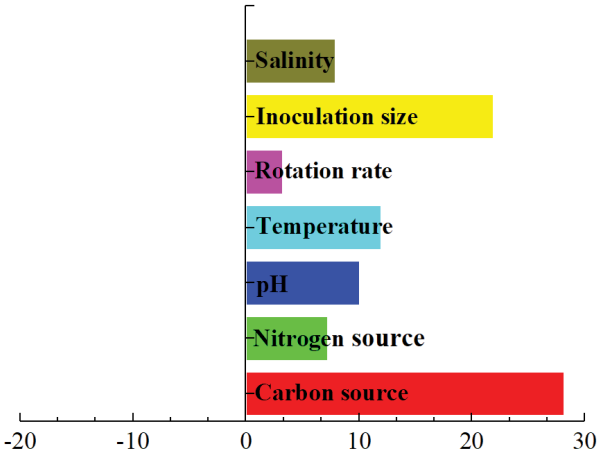

Fig. 1. Estimated effects of seven variables via Plackett–Burman design on Cr(VI) removal.

3.2. Effect of sensitive factors on the model

Experiments were completed to scrutinize the combined effect of four different process parameters on removing Cr(VI) using microbes. The Design Expert software 8 was used to determine the second-order polynomial coefficients for each term of the equation through multiple-regression analysis. All levels like individual factor, interactions, and linear relationship affecting the sensitive factors are shown in Tables 3 and 5. It is revealed that the effects on removal rate of Cr(VI) of factors at linear and quadratic level were shown to be highly-significant.

The improved model equation was used to calculate removal rate of Cr(VI). The quadratic represented the combined effect of all parameters of the model:

$$Y = 87.56 + 4.5A + 2.31B - 3.13C + 6.67D - 0.99AB + 6.43BC - 8.84A^2 - 8.45B^2 - 11.11D^2 \quad (4)$$

where Y is the removal rate of Cr(VI) (%); A, B, C, and D are the coded values of selected factors, carbon source (g L^{-1}), pH, temperature (°C), and inoculation percent (%).

The linear effects, quadratic effects, and interactions between the factors was generated by the form of 3D response surface plot. The center point of pH and carbon source showed the highest response indicating the maximum removal rate of Cr(VI). While the removal rate decreased at the carbon source concentration over 1.8 g.L^{-1}. The concentration of carbon source at 1.8 g.L^{-1} achieved the better removal rate of Cr(VI). The interactions of other factors were similar as the analysis of pH and carbon source. Additionally, as Fig. 2 shows, the red straight line indicated that the internally studentized residuals confirmed a normal distribution. All of points around the straight line had a small amplitude, which implied nearly normal data. The purpose of linear and interaction analysis was to obtain an accurate polynomial function, and composite regression analysis was applied to confirm the model coefficients.

Analysis of variance (ANOVA) was used for testing the adequacy of the developed model and to know the statistical significance of the regression coefficients. In order to confirm significance of the statistical model,

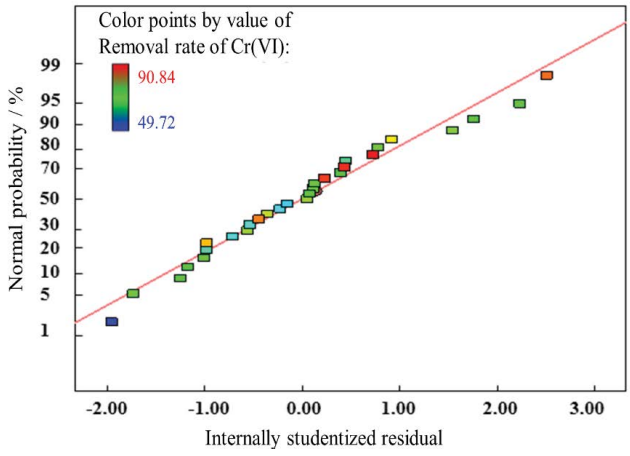

Fig. 2. Normal plot of residuals.

the ANOVA test was carried out and the obtained results are listed in Table 5. The Fischer value of the experimental model (*F*) (27.59) was much higher than the critical *F*-value at a level of 5%. The terms presenting *p*-value lower than 0.05 were significant. These findings indicated that the model was extremely significant with a higher confidence level (99.98%). The lack of fit was 0.1352 (>0.05), suggesting that removal item of the model was not-significant and not missing a valid item. Therefore, the model was considered statistically significant, and it was suitable. The coefficient of determination R^2 = 0.9868 closes to 1.00, in regression equation then the fitted model was considered as highly correlated [41]. In addition, the value of adjusted determination coefficient (Adj. R^2 = 0.9738) was also found acceptable, confirming the model was significant. The value of coefficient of variation (CV = 1.32%) explained that there was superiority in the experimental data and the model, that is, lower value of CV shows high degree of precision (Table 5). Fig. 3 checked the model by coefficient of determination (R^2 = 0.9917) for Cr(VI) removal. Suggesting that all points closed to the straight line revealing significance and accuracy of the model. Therefore, these findings proved the aptness of the predicted model by the BBD for Cr(VI) removal.

3.3. Response surface plotting and removal Cr(VI) optimization

In order to describe the interaction of factors more intuitively, three dimensional response surface plots are shown in Fig. 4. In the model, the carbon source (*A*) was the most significant variable affecting the response, and showed significant interaction with pH (*B*), temperature (*C*), and inoculation percent (*D*). The first graph (Fig. 4a) illustrates the interaction between *A* and *B*. With an increase in *A* from 0.6 to 3.0 at pH 8.0, the removal rate of Cr(VI) improved to 83.40% rapidly. The interactions between variables *A* and *C* are represented in Fig. 4b. The removal rate was found to receive positive influence by a increasing in both *A* concentration and *C* while considering the third factor pH at a constant level of 8.0. A higher value close to 85.6% can be achieved around 1.8 g.L^{-1} of *A*, at

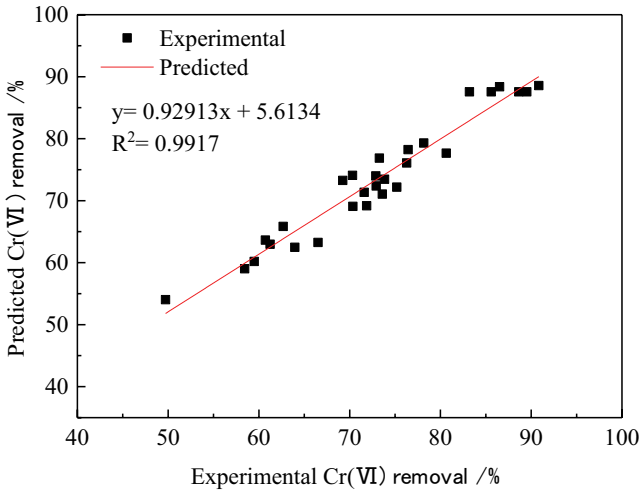

Fig. 3. Comparison of actual and predicted values on Cr(VI) removal.

Table 5
ANOVA for response surface quadratic model

Source	Sum of squares	df	Mean square	*F*-value	*p*-value Prob. > *F*
Model	2,502.00	13	192.46	27.59	0.0002
A–Carbon source (g.L^{-1})	243.00	1	243.00	9.59	0.0074
B–pH	63.85	1	63.85	2.52	0.1333
C–Temperature	117.31	1	117.31	4.63	0.0481
D–Inoculation percent (v/v) (%)	534.40	1	534.40	21.09	0.0004
AB	3.92	1	3.92	0.15	0.6996
BC	165.38	1	165.38	6.53	0.0220
CD	0.44	1	0.44	0.017	0.8974
A^2	506.89	1	506.89	20.00	0.0004
B^2	463.15	1	463.15	18.27	0.0007
C^2	323.31	1	323.31	12.76	0.0828
D^2	800.64	1	800.64	11.59	<0.0001
Residual	380.15	15	25.34		
Lack of fit	341.53	11	31.05	3.22	0.1352
Pure error	38.62	4	9.65		
Cor. total	2,882.15	28			
Standard deviation	5.03		*R*-squared	0.9868	
Mean	72.89		Adj. *R*-squared	0.9738	
C.V. (%)	6.91		Pred. *R*-squared	0.7281	
Press	1,936.53		Adeq. precision	19.015	

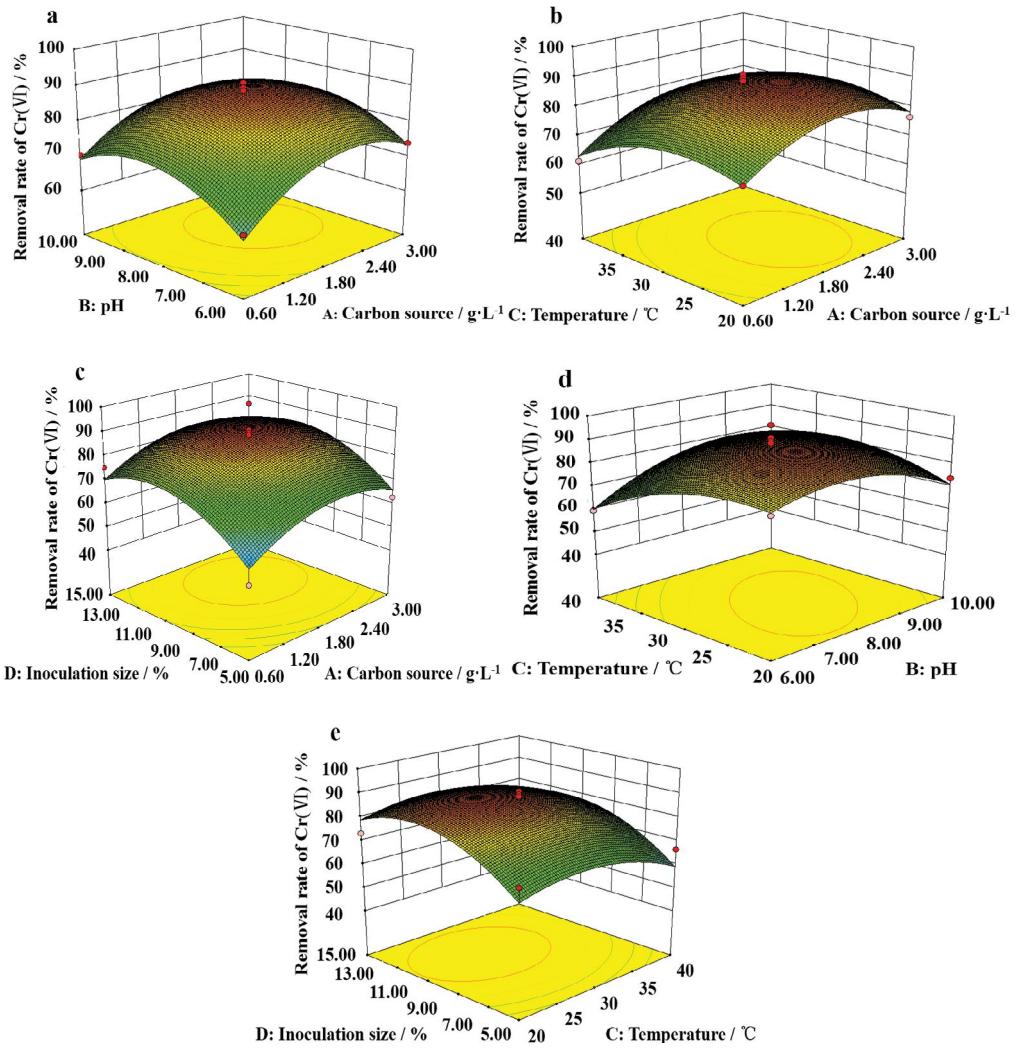

Fig. 4. Response surface plots showing the interactive between carbon source (*A*) pH (*B*), temperature (*C*), and inoculation percent (*D*). Interaction of (a) *A* and *B*, (b) *A* and *C*, (c) *A* and *D*, (d) *C* and *B*, and (e) *C* and *D*.

30°C. A positive relationship of *A* and *D* is shown in Fig. 4c. The Cr(VI) removal efficiency varied greatly (90.84%) in conjunction with the *A* and *D* increasing rapidly. Therefore, the importance of microbial nutrients should be emphasized, as it played a major role to achieve the higher removal rate of Cr(VI). Carbon source have been proved it could be the electron donor providing opportunities for Cr(VI) reduction [10]. At low concentration of carbon source, the activity and population of microorganisms were limited, resulting in the decreased of Cr(VI) removal [30]. On the other hand, Fig. 5d helped to interpret the interaction between factors, *B* and *C* at a constant level of *A* (1.8 g.L^{-1}). The placement of the point of optimization at the center indicated an increasing trend in the value of pH (6–8) from the center point accompanied by *C* of around 25°C–30°C can provide a maximum removal rate of around 89.52%. Likewise, with the increase of *C* and *D* to 30°C, 10%, respectively, the maximum removal rate was up to 88.64% (Fig. 4e).

According to the RSM plots and statistical analysis, a carbon source level of 1.8 g.L^{-1}, pH 8.0, at 30°C, and inoculation percent of 10% were predicted to be an optimal design for enhancement of removal rate of Cr(VI).

3.4. Determination of optimal conditions and validation of model

In order to verify of the optimal condition foretold on Cr(VI) removal by the model, the experiments were performed in triplicates. After optimization of four factors. The microbial culture conditions were set as following: inoculation size 10% (v/v), carbon source 1.8 g.L^{-1}, pH 8.0, and temperature 30°C. The removal rate of Cr(VI) was up to 89.01% for 15 d, and the OD_{600} increased rapidly from 0.20 to 1.38 at the first 10 d (Fig. 5). It was observed that the removal rate of Cr(VI) varied significantly in conjunction with the OD_{600} value increase greatly. Above results were in close consistent with the model prediction, suggesting that this model could well predict the Cr(VI) removal rate by YX-CM. Researchers have proved that the BBD model can accurately predict the biodegradation of atrazine by *Bacillus badius* ABP6 [18].

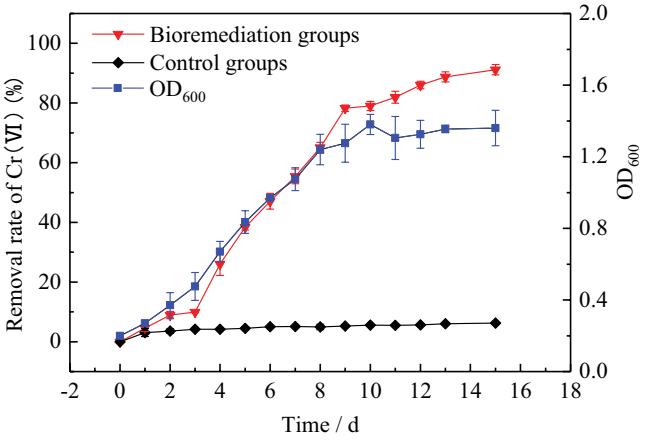

Fig. 5. Validation of Cr(VI) removal by bioremediation under the optimized condition.

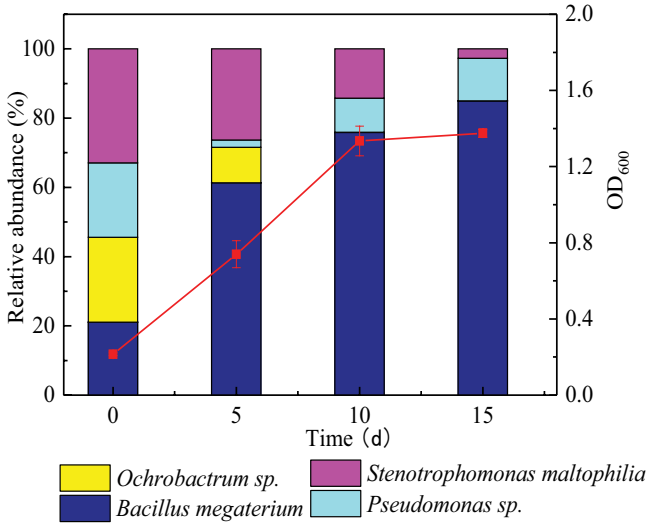

Fig. 6. Relative abundance of each microbial species during bioremediation.

In a comparison with control groups without inoculation microorganisms, the removal rate was only 4.27% (Fig. 5). This can be attributed to biosorption of the organic medium [19,21]. Similar study was also conducted by Vijoyeta and Shubhalakshmi on bioremediation Cr(VI) by *Dmanglicolous* fungi, resulting in a significant rise in removal rate of Cr(VI) by optimizing the important factors [31].

3.5. Microbial community succession

The variation of microbial community structures was significantly correlated with nutritional types of microorganisms and environmental conditions [32]. In this study, data analysis of microbial community succession revealed that the main microbial species (*S. maltophilia*, *Ochrobactrum* sp., *P. putida*, and *B. megaterium*) were always dominant communities (Fig. 6). However, the relative abundance of them varied greatly during bioremediation.

As one of the most abundant microbial species in the natural environment, *Bacillus* sp. has been widely applied to the bioremediation of heavy metals in the contaminated sites [33,34]. In this study, relative abundance of *B. megaterium* increased from 21.07% to 84.96% under the optimal culture conditions. The result can be explained by two factors: the stronger adaptability and competitive. According to the previous studies, the most bacteria could developed various types of resistance mechanisms to adapt to the toxicity of Cr(VI) [35]. The resistant mechanism aided *B. megaterium* to adapt to the new environment rapidly and provide opportunities for reproduction. Numerous studies have confirmed that a positive correlation between Cr(VI) removal efficiency and the population of microorganisms occurred into the bioremediation systems under the suitable nutrients and environmental parameters [16,34]. Simultaneous, other studies support that the harsh environment would stimulate easily the growth and activity of microorganisms to adapt to the present situation [36,37]. Moreover, *B. megaterium*, as gram-positive bacteria, can tolerate higher Cr(VI) concentration and possess stronger competitive due to thicker cell membrane and capsule structure [38]. Therefore, the relative higher abundance of *B. megaterium* during the bioremediation process was reasonable. For *S. maltophilia*, the relative abundance decreased from 32.91% to 2.70% in 15 d. One explanation was that the poor competitive caused microbial death in the new chromium-contaminated environment [28]. The variation of *Ochrobactrum* sp. was significant that it was hardly detected. This result can be related to the poorer competitiveness of *Ochrobactrum* sp. than other [39]. The *P. putida* decreased to 2.132% in the first, then, gradually increased to 12.32%. One of the major reasons for variation of *P. putida* was to adapt to the new Cr(VI) environment for days, and then, *P. putida* was gradual recovery activity in the bioremediation systems. The adaptability and competitiveness of every microbial species had an significant influence on their relative abundance in bioremediation [37]. Finally, in this study, the OD_{600} increased from 0.2 to 1.38 in 10 d, suggesting that the population YX-CM increased rapidly under the optimal culture conditions, and providing enough biological materials for Cr(VI) removal [40,41]. Therefore, together with the variation of removal rate of Cr(VI), these results suggest that the competitiveness and tolerance of different microbial species can be responsible for the changes in relative abundance and ultimately affect microbial community succession in the bioremediation ecosystem [34,39].

3.6. Characterization of precipitated products by SEM-EDS analysis

To further explore the removal mechanism of Cr(VI) by microorganisms, precipitated products after bioremediation were collected to investigate microscopic morphology and main elements by SEM-EDS. The results are illustrated in Fig. 7. As can be seen, clearly visible the products with dark-blue precipitation accumulated in the bottom of centrifugal tube (Fig. 7a). This was due to the Cr(VI) in water-solution transforming into Cr(III)-precipitation (dark-blue) and chromium-chelate compounds [42,43]. The precipitated products existed in various solid structure with different sizes observed by SEM (Fig. 7b). Further analysis of SEM-EDS spectra showed that Cr signals was relative

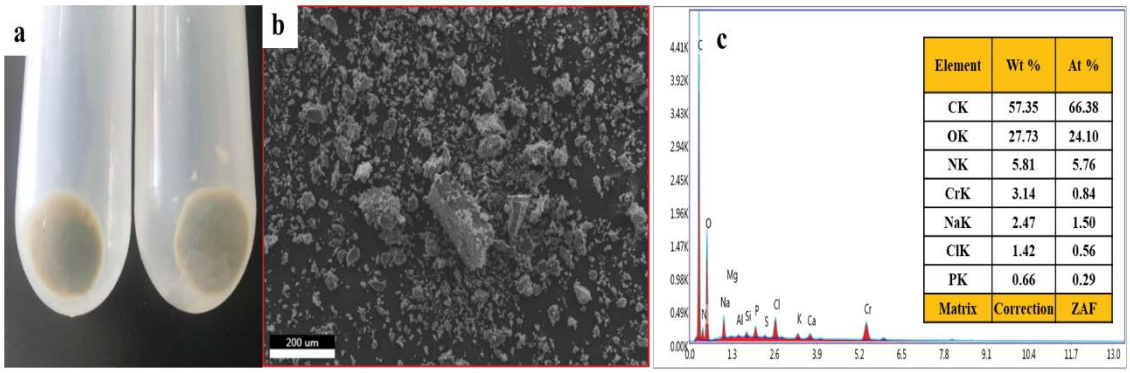

Fig. 7. SEM-EDS analysis of precipitated products: (a) collecting the dark-blue precipitation after centrifugation, (b) SEM images of precipitated products, and (c) EDS analysis of precipitated products.

intensely occurred into the precipitated products, and it was up to 3.14% (Fig. 7c). The appearance of Cr signals in the products indicated that Cr(VI) with higher mobility and solubility was effective limited in the products during the bioremediation process. Similar work was reported that the Cr(VI) in water-solution could transform to precipitations by different bioremediation mechanisms (bioreduction, biosorption, or biomineralizing) [12,16]. On the other hand, the peaks of other major elements, such as C, O, N, P, and S, were also observed, which was related to basic microbial metabolites and microbial composition [44,45].

3.7. Characterization of chromium chemical valence by XPS

In order to determine the chromium speciation after bioremediation of YX-CM, the valence of chromium in the precipitated products was analyzed by XPS [46]. Previous studies confirm that the binding energies in the range of 576.2–576.5 eV of the Cr 2p3/2 orbitals is implied Cr_2O_3 products, and $CrCl_3$ assigns at 577.2 eV [24]. Higher binding energies (585, 588 eV) belong to Cr 2p1/2 orbitals of $Cr(OH)_3$ [47,48]. In this study, the XPS spectrum depicted two peaks at 576.3 and 585.2 eV, indicating Cr(III) products in the precipitated under high-resolution scanning (Fig. 8), which was in agreement with the previous researches suggesting the same Cr(III) binding energy value [49–51]. The results revealed Cr(VI) in water-solution was transformed into Cr(III)-precipitation in the bioremediation process by YX-CM.

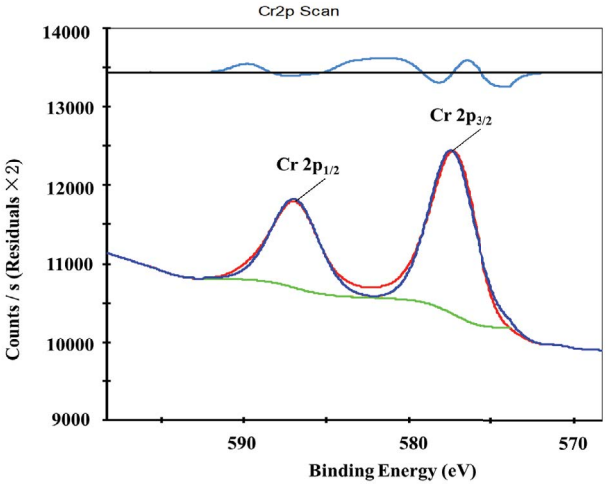

Fig. 8. XPS spectra of high-resolution scan of chromium in precipitated products.

4. Conclusions

This study presented the contribution of important factors to Cr(VI) removal by bioremediation of YX-CM. Carbon source, inoculation percent (v/v), temperature, and pH were screened as the sensitive factors of culture conditions for further study. A RSM-BBD for optimization of microbial culture conditions aimed to improve the removal rate of Cr(VI). The maximum removal rate over 90.84% and microbial optical density (OD_{600}) over 1.36 were obtained under the optimal culture conditions of carbon source of 1.8 $g.L^{-1}$, and inoculation percent (v/v) of 10% when pH at 8.0 and temperature at 30°C. After bioremediation, SEM-EDS and XPS analyses of products demonstrated Cr(VI) with higher mobility and solubility were effective limited and reduced to Cr(III)-precipitation. In addition, microbial community succession revealed that mixed functional microbes (YX-CM) were the dominant flora during the bioremediation. As the most contributor, the relative abundance of *B. megaterium* increased from 21.07% to 84.96%. Finally, it can be concluded that YX-CM can surely be used as an efficient and eco-friendly remediation material which will make more sustainable remove Cr(VI) from the chromium-contaminated sites.

Acknowledgments

This work was supported by the National Natural Science Foundation of China (51974279, U1402234, and 41573074); National Key Research and Development Project of China (2018YFC1802702, 2018YFC1801803, and 2019YFC1805903).

References

[1] M. Shahid, S. Shamshad, M. Rafiq, Chromium speciation, bioavailability, uptake, toxicity and detoxification in soil-plant system: a review, Chemosphere, 178 (2017) 513–533.

[2] C.X. Kang, P.X. Wu, Y.W. Li, Understanding the role of clay minerals in the chromium(VI) bioremoval by *Pseudomonas aeruginosa* CCTCC AB93066 under growth condition: microscopic, spectroscopic and kinetic analysis, World. J. Microbiol. Biotechnol., 31 (2015) 1765–1779.
[3] S. Binoy, N. Ravi, G.S.R. Krishnamurti, Manganese(II)-catalyzed and clay-minerals-mediated reduction of chromium(VI) by citrate, Environ. Sci. Technol., 47 (2013) 13629–13636.
[4] P. Gupta, V. Kumar, Z. Usmani, Phosphate solubilization and chromium(VI) remediation potential of *Klebsiella* sp. strain CPSB4 isolated from the chromium contaminated agricultural soil, Chemosphere, 192 (2017) 318–330.
[5] P.S. González, L.F. Ambrosio, C.E. Paisio, Chromium(VI) remediation by a native strain: effect of environmental conditions and removal mechanisms involved, Environ. Sci. Pollut. Res. Int., 21 (2014) 13551–13559.
[6] R. Xu, K.J. Wu, H.W. Han, Co-expression of YieF and PhoN in *Deinococcus radiodurans* R1 improves uranium bioprecipitation by reducing chromium interference, Chemosphere, 211 (2018) 1156–1165.
[7] C.P. Chen, K.W. Juang, P.D.Y. Lee, Effects of liming on Cr(VI) reduction and Cr phytotoxicity in Cr(VI)-contaminated soils, Soil. Sci. Plant. Nutr., 58 (2012) 135–143.
[8] M.M. Kabir, A.N.M. Fakhruddin, M.A.Z. Chowdhury, Isolation and characterization of chromium(VI)-reducing bacteria from tannery effluents and solid wastes, World J. Microbiol. Biotechnol., 34 (2018) 126–138.
[9] R. Batool, K. Yrjälä, K. Shaukat, Production of EPS under Cr(VI) challenge in two indigenous bacteria isolated from a tannery effluent: EPS production under Cr(VI) stressed condition, J. Basic Microbiol., 55 (2015) 1064–1072.
[10] N.M. Raman, S. Asokan, N.S. Sundari, Bioremediation of chromium(VI) by *Stenotrophomonas maltophilia* isolated from tannery effluent, Int. J. Environ. Sci. Technol., 15 (2017) 207–116.
[11] J. Huang, J. Li, G. Wang, Production of a microcapsule agent of chromate-reducing *Lysinibacillus fusiformis* ZC1 and its application in remediation of chromate-spiked soil, Springerplus, 5 (2016) 561–571.
[12] J.B. Xu, Y.Z. Feng, Y.L. Wang, Effect of Rhizobacterium *Rhodopseudomonas palustris* inoculation on *Stevia rebaudiana* plant growth and soil microbial community, Pedosphere, 28 (2018) 793–803.
[13] K. Sathishkumar, K. Murugan, G. Benelli, Bioreduction of hexavalent chromium by *Pseudomonas stutzeri* L1 and *Acinetobacter baumannii* L2, Ann. Microbiol., 67 (2016) 1–8.
[14] H.Z. Tavakoli, M. Abdollahy, S.J. Ahmadi, The effect of particle size, irrigation rate and aeration rate on column bioleaching of uranium ore, Russ. J. Non-Ferrous Met., 58 (2017) 188–199.
[15] A. Hauwa, R. Mohamed, A. Al-Gheethi, Harvesting of *Botryococcus* sp. biomass from greywater by natural coagulants, Waste Biomass Valorization, 9 (2017) 1841–1853.
[16] A.A. Gheethia, E. Noman, R.M.S.R. Mohameda, Optimizing of pharmaceutical active compounds biodegradability in secondary effluents by β-lactamase from *Bacillus subtilis* using central composite design, J. Hazard. Mater., 365 (2019) 883–894.
[17] K. Kalantari, M. Ahmad, H. Masoumi, Rapid adsorption of heavy metals by Fe_3O_4/talc nanocomposite and optimization study using response surface methodology, Int. J. Mol. Sci., 153390 (2014) 12913–12927.
[18] H. Khatoon, J.P.N. Rai, Optimization studies on biodegradation of atrazine by *Bacillus badius* ABP6 strain using response surface methodology, Biotechnol. Rep., 1 (2020) 446–459.
[19] H. Li, V.D.D. Sander, F. Bunge, Optimization of on-chip bacterial culture conditions using the Box–Behnken design response surface methodology for faster drug susceptibility screening, Talanta, 194 (2019) 627–633.
[20] A.C. Rodrigues, A.I. Fontão, A. Coelho, Response surface statistical optimization of bacterial nanocellulose fermentation in static culture using a low-cost medium, New Biotechnol., 21 (2018) 1536–1542.
[21] J. Zhang, Y.C. Dong, L.L. Fan, Optimization of culture medium compositions for gellan gum production by a halobacterium *Sphingomonas paucimobilis*, Carbohydr. Polym., 115 (2015) 694–700.
[22] A. Pandey, A. Gupta, A. Sunny, Multi-objective optimization of media components for improved algae biomass, fatty acid and starch biosynthesis from *Scenedesmus* sp. ASK22 using desirability function approach, Renewable Energy, 150 (2020) 476–486.
[23] Y. Wang, P. Bing, Z. Yang, Bacterial community dynamics during bioremediation of Cr(VI)-contaminated soil, Appl. Soil. Ecol., 85 (2015) 50–55.
[24] J. Xie, J. Lin, X. Zhou, pH-dependent microbial reduction of Uranium(VI) in carbonate-free solutions: UV-vis, XPS, TEM, and thermodynamic studies, Environ. Sci. Pollut. Res., 25 (2018) 22308–22317.
[25] G. Chen, J. Han, Y. Mu, Two-stage chromium isotope fractionation during microbial Cr(VI) reduction, Water Res., 148 (2018) 10–18.
[26] Q. Zhang, K. Amor, S.J.G. Galer, Variations of stable isotope fractionation during bacterial chromium reduction processes and their implications, Chem. Geol., 481 (2018) 155–164.
[27] X.N. Huang, D. Min, D.F. Liu, Formation mechanism of organo-chromium(III) complexes from bioreduction of chromium (VI) by *Aeromonas hydrophila*, Environ. Int., 129 (2019) 86–94.
[28] Y.E. Zhu, H. Li, G.X. Zhang, Removal of hexavalent chromium from aqueous solution by different surface-modified biochars: acid washing, nanoscale zero-valent iron and ferric iron loading, Bioresour. Technol., 261 (2018) 142–150.
[29] A. Hedayatkhah, M.S. Cretoiu, G. Emtiazi, Bioremediation of chromium contaminated water by diatoms with concomitant lipid accumulation for biofuel production, J. Environ. Manage., 227 (2018) 313–320.
[30] A.V. Schenone, L.O. Conte, M.A. Botta, Modeling and optimization of photo-Fenton degradation of 2,4-D using ferrioxalate complex and response surface methodology (RSM), J. Environ. Manage., 155 (2015) 177–183.
[31] C. Vijoyeta, S. Shubhalakshmi, C. Punarbasu, Assessment on removal efficiency of chromium by the isolated *manglicolous* fungi from Indian Sundarban mangrove forest: removal and optimization using response surface methodology, Environ. Technol. Innovation, 10 (2018) 335–344.
[32] J.T.E. Lee, Q.K. Wang, E.Y. Lim, Optimization of bioaugmentation of the anaerobic digestion of *Axonopus compressus* cowgrass for the production of biomethane, J. Cleaner Prod., 258 (2020) 1209–1232.
[33] G. Fierrosromero, M. Gómezramírez, G.E. Arenasisaac, Identification of *Bacillus megaterium* and *Microbacterium liquefaciens* genes involved in metal resistance and metal removal, Can. J. Microbiol., 62 (2016) 505–513.
[34] S. Das, J. Mishra, S. K. Das, Investigation on mechanism of Cr(VI) reduction and removal by *Bacillus amyloliquefaciens*, a novel chromate tolerant bacterium isolated from chromite mine soil, Chemosphere, 96 (2014) 112–121.
[35] R. Jobby, P. Jha, A.K. Yadav, Biosorption and biotransformation of hexavalent chromium [Cr(VI)]: a comprehensive review, Chemosphere, 207 (2018) 255–266.
[36] X.Q. Zhao, J. Huang, J. Lu, Study on the influence of soil microbial community on the long-term heavy metal pollution of different land use types and depth layers in mine, Ecotoxicol. Environ. Saf., 170 (2019) 218–226.
[37] R.E. Beattie, H. Wyatt, M.F. Campa, Variation in microbial community structure correlates with heavy-metal contamination in soils decades after mining ceased, Soil Biol. Biochem., 126 (2018) 57–63.
[38] F. Vendruscolo, G.L.D.R. Ferreira, N.R.A. Filho, Biosorption of hexavalent chromium by microorganisms, Int. Biodeterior. Biodegrad., 119 (2016) 87–95.
[39] B. Liu, G. Su, Y.R. Yang, Vertical distribution of microbial communities in chromium-contaminated soil and isolation of Cr(IV)-reducing strains, Ecotoxicol. Environ. Saf., 180 (2019) 242–251.
[40] H. Huang, K. Wu, A. Khan, A novel *Pseudomonas gessardii strain* LZ-E simultaneously degrades naphthalene and reduces hexavalent chromium, Bioresour. Technol., 207 (2016) 370–378.

[41] R.N. Bharagava, S. Mishra, Hexavalent chromium reduction potential of *Cellulosimicrobium* sp. isolated from common effluent treatment plant of tannery industries, Ecotoxicol. Environ. Saf., 147 (2018) 102–109.
[42] D. Long, X. Tang, K. Cai, Cr(VI) resistance and removal by indigenous bacteria isolated from chromium-contaminated soil, J. Microbiol. Biotechnol., 23 (2013) 1123–1132.
[43] A. Elahi, A. Rehman, Comparative behavior of two gram positive Cr^{6+} resistant bacterial strains *Bacillus aerius* S1 and *Brevibacterium iodinum* S2 under hexavalent chromium stress, Biotechnol. Rep., 21 (2019) 1–8.
[44] Y. Gong, C.J. Werth, Y. He, Intracellular versus extracellular accumulation of Hexavalent chromium reduction products by *Geobacter sulfurreducens* PCA, Environ. Pollut., 240 (2018) 485–492.
[45] D.C. Prabhakaran, S. Subramanian, Studies on the bio-remediation of chromium from aqueous solutions using *C. paurometabolum*, Trans. Indian Inst. Metals, 70 (2016) 497–509.
[46] Z. Chen, S. Song, Y. Wen, Reduction of Cr(VI) into Cr(III) by organelles of *Chlorella vulgaris* in aqueous solution: an organelle-level attempt, Sci. Total Environ., 572 (2016) 361–368.
[47] Y.P. Xie, H. Li, X.W. Wang, Kinetic simulating of Cr(VI) removal by the waste *Chlorella vulgaris* biomass, J. Taiwan Inst. Chem. Eng., 45 (2014) 1773–1782.
[48] Q. Zeng, Y. Hu, Y. Yang, Cell envelop is the key site for Cr(IV) reduction by *Oceanobacillus oncorhynchi* W4, a newly isolated Cr(IV) reducing bacterium, J. Hazard. Mater., 368 (2019) 149–155.
[49] M. Gan, C.Y. Gu, J.J. Ding, Hexavalent chromium remediation based on the synergistic effect between chemoautotrophic bacteria and sulfide minerals, Ecotoxicol. Environ. Saf., 173 (2019) 118–130.